Implementation of Uncertainty Analysis for Evaluation of Nuclear Reactors VVER-1000 Fuel Safety Margins during Normal Operation by FEMAXI-6 Computer Code Calculations

Venelin Rusanov[1], Plamen V. Petkov[2] and Krassimir Kamenov[3]

[1]*Department of Nuclear Engineering, Faculty of Physics, Sofia University "St. Kliment Ohridski" , 1164 Sofia, Bulgaria*
[2]*Department of Nuclear Engineering, Faculty of Physics, Sofia University "St. Kliment Ohridski" , 1164 Sofia, Bulgaria*
[3]*Kozloduy NPP Plc., 3321 Vratsa, Bulgaria*

Abstract. The mathematical modelling and evaluation of the nuclear fuel while burning in nuclear reactors is of significant importance if one wants to predict the reactor core behavior and to get assured that the necessary criteria for its safe operation are met. These criteria reflect the maximum fuel temperature, cladding temperature, coolant heating, etc. The computer code that we chose for performance of such analysis is FEMAXI-6 (Japan Atomic Energy Agency). We prepared input-data deck for fuel rods of the type used in Kozloduy NPP and performed predictive calculations for the evaluation of the safety margins. However, for the proper evaluation it is important to know the initial geometrical and material data. These data are available only through their nominal values and uncertainty ranges, given by the fuel vendor as the fuel itself is sealed in tubes, made of zirconium alloy. Therefore, the lack of knowledge about the exact values of these important characteristics requires the implementation of an uncertainty analysis in order to evaluate properly the safety criteria.
As a rule, the uncertainty analyses are applied for evaluation of margins in safety analyses, performed for transients and accidents. There are several known methods for performance of such analyses. One of them is the method, developed by GRS (Gesellschaft für Anlagen- und Reaktorsicherheit) and implemented in SUSA (Software for Uncertainty and Sensitivity Analyses). We tested successfully the Wolfram Mathematica's capability to implement the same approach by analysis of the two, most heavily loaded fuel rods in the reactor core (containing correspondingly UO_2 and $UO_2 - Gd_2O_3$ fuel) during normal reactor operation. Finally, the following conclusion about this fuel is made: its operation in thermo-mechanical and thermo-hydraulic aspects is safe. The safety criterion: critical heat flux ratio (CHFR) is met.

Keywords: nuclear, uncertainty, VVER-1000, WWER-1000, FEMAXI-6, TRANSURANUS, Wilks, CHF, Wolfram Mathematica

1. INTRODUCTION

Currently, the pressurized water reactors (PWR) are the most popular design for commercial electricity production from nuclear power. The Russian design (VVER-1000) that has an electrical output of 1000 MW, has recently been subject to power uprate and extension of the fuel cycle (Molchanov, 2009). The margins to important safety limits (such as critical heat flux), are decreased but this is acceptable because of the improvement of the overall knowledge about the ongoing processes in operation and the advancement in understanding of the properties of irradiated materials. This requires the implementation of newer, improved analytical approaches for the estimation of the behavior of the nuclear fuel that involve not only neutron-diffusion but also thermo-mechanical and thermo-physical aspects.

The smallest replaceable fuel component of nuclear reactor cores is the fuel assembly

(Onufriev, 2005). Each fuel assembly consists of 306 heat generating fuel rods containing UO_2 and six fuel rods with $UO_2 - Gd_2O_3$ mixture. The reactor core consists of 163 fuel assemblies. Their reloading takes place every year after reactor shutdown for refueling. The removed most burned fuel assemblies are replaced with fresh ones (Kamenov, 2012).

For the performance of the current analysis FEMAXI-6 computer code, obtained from NEA (Nuclear Energy Agency) database (OECD, 2017), was used as a main tool, along with scripts that we prepare in Wolfram Mathematica scripting language (Wolfram Research Inc., 2016) and an additional computer program that we wrote in FORTRAN. This computer program models PG-correlation, (Pernica & Cizek, 1995) for the estimation of the margins to the critical heat flux: departure from nucleate boiling ratio (DNBR).

The input data for the current analysis, such as irradiation history, power peaking (non-uniformity) factors, coolant inlet temperature, etc., were prepared in "Kozloduy NPP" as part of an optimization process for finding the most economically favorable core loading for a four-year fuel cycle, (Kamenov, 2017). The cases selected for the current analysis, are the most unfavorable ones with respect to the economical and physical reactor core behavior. For them the highest power peaking (non-uniformity) factors were predicted. Because of this, the most unfavorable loading was never physically realized during plant operation but is suitable for theoretical analyses.

2. THEORETICAL BASIS

In the case of VVER-1000 (operated in Kozloduy NPP, Bulgaria), the importance of geometrical, material, etc. uncertainties during normal operation should be clarified. Therefore, the goal of the presented study in the paper is to estimate the influence of the initial uncertainties resulting from the fuel fabrication on the fuel behavior during normal operation in the reactor core. The performance of the analysis does not require investigation of the entire reactor core that contains 50856 fuel rods. It is enough to select the two, most heavily loaded by thermal power fuel rods: one of them containing UO_2 and the second one containing $UO_2 - Gd_2O_3$ mixture.

Both types of fuel rods are made of pellets with an outer diameter, d_{fuel}^{out}= 7.57 mm and a fuel pellet gap diameter, d_{fuel}^{in}= 1.4/1.5 correspondingly for $UO_2/UO_2 - Gd_2O_3$. The pellets have a height of 10 mm. They are placed and sealed in a vertical column within cylindrical rods of 0.685 mm thickness, made of zirconium alloy with 1% Nb (called E110). The length of the fuel rod is 3.53 m and its outer diameter, d_{cl}^{out} is 9.10 mm, (Onufriev, 2005; Kamenov, 2017; Kovbasenko, 2016), see Table 1. The concentration of Gd_2O_3 is up to 5%, (Kamenov, 2017; Odeychuk et al, 2008). Initially, a gap exists between the cladding and the fuel column, filled with pure helium under 2.0 MPa pressure at room temperature (Onufriev, 2005). The sketch in Fig. 1 (the horizontal cross-section), gives an additional clarification of the geometrical parameters.

The six important parameters (for each type of fuel rod), subject to the analysis, and their initial uncertainty ranges (lower and upper bounds) are given in Table 1 (Kovbasenko, 2016):

1. Initial fuel pellet gap diameter: $d_{fuel}^{in}(UO_2)/d_{fuel}^{in}(UO_2 - Gd_2O_3)$;
2. Initial fuel pellet outer diameter: $d_{fuel}^{out}(UO_2)/d_{fuel}^{out}(UO_2 - Gd_2O_3)$;
3. Initial cladding inner diameter: $d_{cl}^{in}(UO_2)/$ $d_{cl}^{in}(UO_2 - Gd_2O_3)$;
4. initial cladding outer diameter: $d_{cl}^{out}(UO_2)/$ $d_{cl}^{out}(UO_2 - Gd_2O_3)$;
5. Initial fuel pellets material density: $\rho_{fuel}(UO_2),/\rho_{fuel}(UO_2 - Gd_2O_3)$ is the amount of mass per unit volume at room temperature;
6. Initial gas pressure within the fuel rod. $p_{gas}(UO_2)/\, p_{gas}(UO_2 - Gd_2O_3)$.

The relative uncertainties of these six parameters (regarding the nominal values), are shown in Fig. 2. The data indicate that the biggest uncertainty exists for the initial gas

pressure (~24%) and the fuel pellet gap diameter, (14%). The remaining parameters show relative deviation less than 4%. The smallest variation is for the fuel pellet outer diameter, only 0.4%.

For a better understanding of the fuel behavior, three more parameters are added in the sensitivity analysis both for UO_2 and $UO_2 - Gd_2O_3$ fuel rods:

7. Initial thickness of the fuel pellet, defined as: $\frac{\left(d_{fuel}^{out} - d_{fuel}^{in}\right)}{2}$;
8. Initial thickness of the gap: $\frac{\left(d_{cl}^{in} - d_{fuel}^{out}\right)}{2}$;
9. Initial thickness of the cladding wall: $\frac{\left(d_{cl}^{out} - d_{cl}^{in}\right)}{2}$;

The initial values of these additional parameters are not varied independently, but are derived from the values of input parameters 1 to 6 (Figs. A3&A6).

The average Spearman's coefficient (No.10 in Figs. A3 & A6) presents the average values of correlation coefficient for first six input parameters (from 1 through 6). Its purpose is to show the overall sufficiency of the number of the analyzed parameters. In Figs. A3 & A6, it is seen that in most of the cases it is close to zero that indicates the balance of the selection of the parameters.

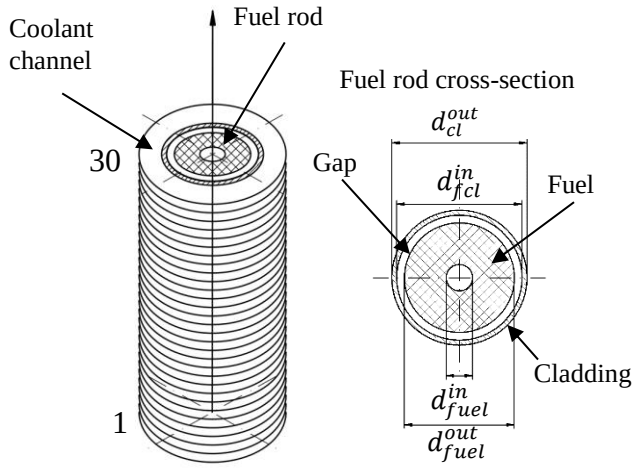

Fig. 1 Nodalization scheme for FEMAXI-6 calculations.

2.1 Analytical procedure

The analytical procedure includes the following major consecutive steps:

1. Development of two basic input data sets correspondingly for $UO_2/UO_2 - Gd_2O_3$ fuel rods, for FEMAXI-6 calculation. Each of these input data sets is replicated later 100 times with variated input values within the uncertainty ranges (Table 1);
2. Performance of 2×101 calculations (for two fuel rods) in order to create the corresponding sets of output values (vectors) for the selected operational parameters;
3. Analysis of uncertainties, based on the published algorithms by Gesellschaft für Anlagen- und Reaktorsicherheit (GRS) gGmbH and implemented by them in a package, called Software for Uncertainty and Sensitivity Analyses (SUSA), Glaeser, (2008) and Kloos, (2015). The final goal is to determine the most favorable and unfavorable cases of random input parameters combination, giving with a certain probability the limits;
4. Evaluation of the critical heat flux (CHF) margin for the most unfavorable case (for the selected fuel rods), using the PG correlation (Pernica & Cizer, 1994). The obtained results at this step are bounding for the entire reactor core.

2.2 Development of a model of fuel rods for FEMAXI-6

The Japan Atomic Energy Agency (JAEA) developed the FEMAXI-6 computer code (Suzuki & Saitou, 2005). The code is capable of performing thermo-mechanical and heat transfer calculations during normal operation and transient conditions of fuel rods. The program can simulate heat transfer; spatial distribution of heat flux; thermally induced corrosion; components elongation; elastic and plastic deformations; processes of cracking, relocation, densification and swelling. Models for cladding-pellet interaction are implemented too. The proper usage of the program requires development of the input data set that correctly

reflects the geometrical and physical properties of VVER-1000 fuel rods. The required input data are taken for the following two fuel rods, irradiated four years in the reactor core (Kamenov, 2017):

- UO_2: 4.0% enriched fuel rod with maximum burnup of 60.83 MW.d/kgU at the end of its four-year cycle;
- $UO_2 - Gd_2O_3$: 3.6% enriched fuel rod with maximum burnup 56.31 MW.d/kgU at the end of its four-year cycle;

The options of the FEMAXI-6 computer code are selected as recommended in Suzuki & Saitou (2005), for modelling the standard phenomena that take place during the fuel operation in a reactor core (USNRC TREE NUREG, 1976; Fukushima et al., 1982; Wiesenack, 2000; Schrire et al., 1998).

The fuel channel nodalization scheme is presented in Fig. 1. The fuel rod is divided into 30 axial layers. The flowing coolant shell around it forms the coolant channel accounted for in the model. The hydraulic diameter of the channel is estimated to be 1.145 cm. The water-covered area is 0.753 cm^2.

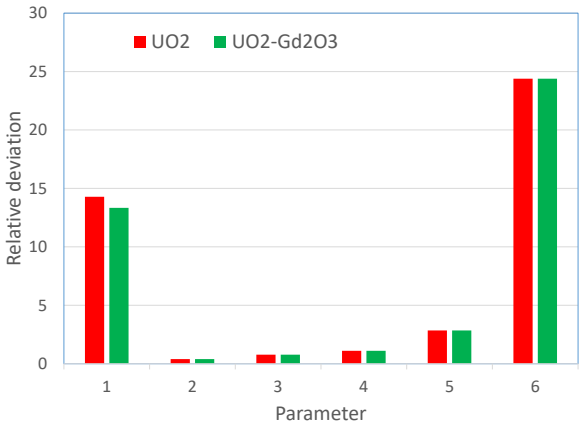

Fig. 2 Relative deviation of the investigated parameters form their nominal values for two fuel rods: 1- fuel pellet gap diameter; 2- fuel pellet outer diameter; 3- cladding inner diameter; 4- cladding outer diameter; 5- fuel pellet material density; 6- initial gas pressure within the fuel rod.

The column of fuel pellets is divided into 5 radial rings in FEMAXI-6 numerical scheme. The cladding of the fuel rods is divided into 2 numerical rings. Two oxide layers on the cladding are also accounted for, correspondingly at the inner and outer sides (Suzuki & Saitou, 2005).

The axial numbering of the nodes starts from the lowest level (Fig. 1), because the coolant enters the fuel rod channel from the bottom.

The considered coolant boundary conditions are as follows: the inlet temperature is 290 °C and the pressure in the coolant channel, is 15.7 MPa.

2.3 Uncertainty and sensitivity analysis

The application of the SUSA method includes four stages:

(1) Determination of potentially important for the output results initial parameters that have defined uncertainty. The selected parameters are given in Table 1 and Fig. 2. Based on the available expertise, the most appropriate statistical distribution for them is Gaussian (Normal). Nevertheless, we assumed uniform probability density function (PDF) of the six input parameters mentioned above, where each value between the lower and upper bounds has an equal probability to occur (Table 1, Glaeser, 2008). This is done in order to reveal better, the relationships between the input and output parameters. We perform nonparametric statistical analysis applying Spearman's correlation, and what appears important is not the frequency of appearance of a given value but the overall level of monotonicity between the input and output parameters (Glaeser, 2008).

TABLE 1. Nominal values, uncertainty ranges and assumed probability distributions of the input parameters.

No.	Parameter	units	Nominal value	Lower bound	Upper bond	Distribution
1	$d_{fuel}^{in}(UO_2)$	*cm*	0.14	0.14	0.16	Uniform

2	$d_{fuel}^{out}(UO_2)$	*cm*	0.757	0.754	0.757	Uniform
3	$d_{cl}^{in}(UO_2)$	*cm*	0.773	0.773	0.779	Uniform
4	$d_{cl}^{out}(UO_2)$	*cm*	0.91	0.905	0.915	Uniform
5	$\rho_{fuel}(UO_2)$	*kg/m*^{3}	10.55	10.4	10.7	Uniform
6	$p_{gas}(UO_2)$	*MPa*	2.05	1.8	2.3	Uniform
7	$d_{fuel}^{in}(UO_2 - Gd_2O_3)$	*cm*	0.15	0.15	0.17	Uniform
8	$d_{fuel}^{out}(UO_2 - Gd_2O_3)$	*cm*	0.757	0.754	0.757	Uniform
9	$d_{cl}^{in}(UO_2 - Gd_2O_3)$	*cm*	0.773	0.773	0.779	Uniform
10	$d_{cl}^{out}(UO_2 - Gd_2O_3)$	*cm*	0.91	0.905	0.915	Uniform
11	$\rho_{fuel}(UO_2 - Gd_2O_3)$	*kg/m*^{3}	10.55	10.4	10.7	Uniform
12	$p_{gas}(UO_2 - Gd_2O_3)$	*MPa*	2.05	1.8	2.3	Uniform

(2) Generation in a random way (with the desired PDF), of *n* vectors of values of the initial parameters and placing them within *n* input data sets for each fuel rod, i.e. 2*n* vectors for both fuel rods and *2n* input data sets. The number of the vectors is determined by the Wilks formula (Wilks, 1941; Wilks, 1942):

$$1 - \left(\frac{u}{100}\right)^n \geq \frac{v}{100} \qquad (1)$$

The meaning of the formula is that *n* calculations are enough for the prediction of a random distribution maximum response with a confidence level, *u* and probability, *v* (Note that the formula is independent from the assumption of the initial probability distribution). The minimum number of calculations is determined from the data in Table 2, based on Eq. 1. We generated 98 combinations of parameters. According to the data in Table 2, this number of runs guarantees the confidence level 95% and 95% probability. We added to them two boundary cases: the most optimistic and the most pessimistic, estimated by expert considerations (see Ch. 3) and the basic case with the nominal values, given in Table 1.

TABLE 2. Number of calculations *n*, estimated by the Wilks formula.

v, %/u, %	90	95	99
90	38	77	388
95	46	**93**	473
99	64	130	662

We prepared 98 input vectors with variated parameters from Table 1. The Wolfram Mathematica script that we wrote previously, fully automated the process of vector generation.

(3) Uncertainty analysis: calculation of output parameters by FEMAXI-6 computer code for 101 cases. In the end, for every input vector we obtained a set of output parameters. The obtained maximal and minimal values (or time trends) of an output parameters give the bounds inside which with 95% probability will lie 95% of all possible combinations of the input parameters, varied inside their uncertainty ranges;

TABLE 3. Quantitative estimation of the power of Spearman correlation coefficient.

No	Range	Relation
1	0.00 – 0.19	Very weak
2	0.20 – 0.39	weak
3	0.40 – 0.59	average
4	0.60 – 0.79	strong
5	0.80 – 1.0	Very strong

(4) Sensitivity analysis: statistical analysis following the method and the algorithm implemented in SUSA. Our current analysis is based on the Spearman's correlation coefficient, r_s: $-1 \leq r_s \leq 1$. It defines a statistical relationship between the input and output parameters. The strength of monotonicity is estimated similarly to the well-known Pearson correlation coefficient but without the assumption for the normality of the initial PDF (Table 3).

Our Wolfram Mathematica script performed statistical analysis following the exact procedure, implemented in SUSA. The

formula, called by the script, is the following (see for example Conover, 1999):

$$r_s = 1 - \frac{6\sum D_i}{n(n^2-1)} \qquad (2)$$

Where n is the number of pairs in the created rank, and D_i is the difference between *i-th* pair of values in the rank.

The aim of the analysis is to evaluate the influence of the input parameters to the uncertainty of the output parameters.

2.4 Input Data Set Verification

The verification procedure is an important step in an input data set development, because it confirms that the results from the prepared sets of data are reliable. The verification of FEMAXI-6 is reported in variety of sources (IAEA, 2013; Passage et al. 2009; Udagawa et al., 2007 and Yamaji et al., 2009). This verification covers mostly the computer code models. Our independent verification is performed particularly with the prepared input data set for VVER-1000 fuel rods. We did the verification with a reported calculation for the same fuel rods (subject to the current analysis) by the TRANSURANUS computer code, (Stefanova et al., 2012).

The compared data of the parameter: temperature at the inner surface of the fuel pellet, show in our further analysis sufficient sensitivity to the initial uncertainty.

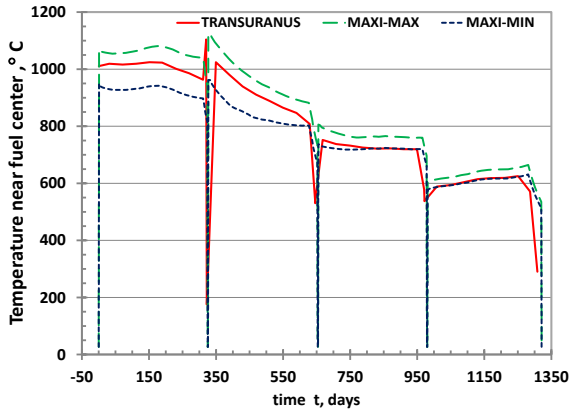

Fig. 3 Verification of UO_2 fuel rod input data for FEMAXI-6 with TRANSURANUS calculation.

The calculation of TRANSURANUS with nominal input values (Table 1) was compared with the highest and the lowest bounding curves of the output uncertainty range produced by FEMAXI-6 (the most optimistic and the most pessimistic cases). The same linear heat generation rate and outer side cladding temperatures were used as boundary conditions in the calculations, performed by the two programs. These data, used in the analysis, were prepared in Kozloduy NPP, (Kamenov, 2017).

The results in Figs. 3 & 4 are for axial layer No. 14, where the highest linear heat generation rate is predicted. These results indicate that the most optimistic and the most pessimistic curves, produced by FEMAXI-6, bound the TRANSURANUS calculation during the most of the operational time.

Considering the evaluation of the uncertainties and the TRANSURANUS input data set previous verifications (Stefanova et al., 2005), the comparison between the results from the two codes indicate that our input data set for FEMAXI-6 code can predict sufficiently accurate the VVER-1000 fuel rods behavior. We came to a conclusion that our input data set is suitable for further reactor core analyses.

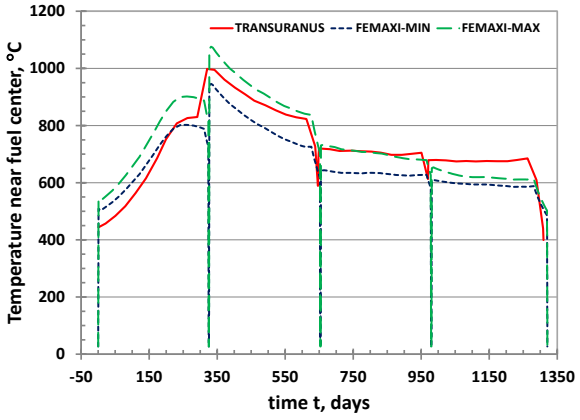

Fig. 4 Verification of $UO_2 - Gd_2O_3$ fuel rod input data for FEMAXI-6 with TRANSURANUS calculation.

2.5 Output Parameters

The subject of the analysis is the following output parameters for $UO_2/UO_2 - Gd_2O_3$ fuel rods (marked with the corresponding letter in Figs. A1÷A6):

a) Temperature at the inner surface of the fuel pellet (pellet center temperature);
b) Temperature in the cladding (cladding nodal temperature);
c) Coolant temperature;
d) Mechanical parameter, presenting the thickness of the gap between the cladding and the fuel pellet: $d_{cl}^{in} - d_{fuel}^{out}$ (thermal diameter gap);
e) Outer diameter of the cladding (cladding outer diameter).
f) Gas pressure (note: because of the gas fission products release, the composition of the gas changes during the fuel cycle);

The above-mentioned six output parameters are analyzed statistically by the Spearman's nonparametric approach.

2.6 Evaluation of the Margin to the CHF

The knowledge of the departure from nucleate boiling (DNB or CHF) known as 'crisis of the first kind' is a very important for safety operation of nuclear facilities, (Tong, 1997). It is characterized by an appearance of heat flux reduction that cannot be easily predicted. The current knowledge allows implementing some empirical correlations that resulted from experimental observations. During the normal power plant operations, the coolant removes the generated heat from the fuel rods. If the heat flux is strong enough, then some local, near to the rods surfaces subcooled boiling can take place. If the void fraction is significant and a film of steam covers the surface of the rod, then the heat removal is reduced and DNB critical regime takes place.

The PG-correlation is valid for all pressurized reactors. It has a general structure as follows (Pernica & Cizek, 1994):

$$CHFR = f\left(P_r, G, x_i, x, q, dT_r, F_g\right) = \frac{k_1}{f(P)_r}\frac{F_g}{(dT_r)^{k_2}}\frac{f(P_r,G)f(P_r,x_i)}{f_a} \quad (3)$$

Where:

- $P_r = {}^{P}/_{22.115}$ is the reduced pressure of the coolant (P is in MPa);
- G is the mass flow rate of the coolant, kg/s;
- x_i is the coolant input void fraction in the channel;
- x is the local void fraction in the point of the expected CHF;
- q is the local heat flux in the point of expected CHF;
- dT_r consists of two multiplied values:
  - d – equivalent diameter, m:
    $$d = \frac{4A}{\sum_i r_i} \quad (4)$$
    Where:
    A is the effective area of the cooling fluid (channel), m^2;
    r_i is the geometry perimeter, m;
  - T_r is a form factor for radial distribution of the heat flux:
    $$T_r = q\frac{\sum_i r_i}{\sum_i r_i q_i} \quad (5)$$
    Where:
    q is the local heat flux for a given perimeter, *W/(m.K)*;
    r_i is the perimeter i, m;
    q_i is the heat flux i in perimeter r_i, *W/(m.K)*;
- F_g is a geometrical factor.

The dimensionless term CHFR (Critical Heat Flux Ratio) is the ratio of the critical heat flux to the current heat flux. The boiling crisis is avoided if CHFR is greater than one. For a correct evaluation of this parameter, the PG-correlation is implemented in the FORTRAN program. The input data for this calculation are the most conservative results from FEMAXI-6 (the most pessimistic data).

3 ANALYTICAL RESULTS

We obtained the results in Figs. A1-A6 after usage of 98 vectors of statistically

random input data, taking account of the input uncertainty ranges (Table 1). The systematic analysis of the results of the calculations reveals that the most interesting axial layer is No. 14, because the highest value of linear power is observed there.

The parameters shown in Figs A1 a)-1, 2 and A4 a)-1, 2 reveal that the temperature at the inner surface of the fuel pellets varies in a range bigger than 200 °C. The temperatures in the cladding vary significantly less, around 10-15 °C, as seen in Figs. A1 b)-1, 2 and A4 b)-1, 2. Finally, the uncertainty in the coolant temperature is only 1-2 °C, observed in Figs A1 c)-1, 2 and A4 c)-1, 2. The effect is explained by the high specific heat capacity of UO_2. In the range 900-1200°C it increases relatively slowly with the increasing of the temperature, and it reflects the transferred heat variation to the outer surface of the cladding (Esser et al., 2014). In Figs A2 d)-1, 2 and A5 d)-1, 2 one can see the response of the gap closure to the initial uncertainties. The difference between the earliest and latest moments of the gap closure is almost 400/624 days. The radial displacement of the outer side of the cladding is around -90/-70 μm (UO_2/$UO_2 - Gd_2O_3$), Figs. A2, e)-1, 2 and A5 e)-1, 2 correspondingly at 550/1000 day of fuel irradiation.

A significant variation of the internal gas pressure is observed, (Figs. A2 f)-1,2 and A5 f)-1,2). It remains below the coolant pressure, which resulted in negative change of the cladding outer diameter.

Therefore, the initial uncertainties of the fuel rod reflect mostly the mechanical properties of the fuel rods rather than the thermo-physical ones.

The monotonic relation between the input uncertainties and those of the selected output parameters is of significant interest. These results are presented in Fig. A3 for UO_2 fuel rod and in Fig. A6 for $UO_2 - Gd_2O_3$ fuel rod for characteristic moments of fuel operation in the reactor core:

a) Maximum temperature at the inner surface of the fuel pellet at 331.92/331.92 day;
b) Maximum temperature in the cladding, at 331.92/331.92 day;
c) Average coolant temperature at 331.92/331.92 day;
d) Biggest gap between the cladding and the fuel pellet at 1.0/1.0 day;
e) Biggest deformation of the average cladding diameter at 660.12/652.12 day of irradiation;
f) Maximum average gas pressure at 660.12/986.07 day.

It is seen from Figs. A3 a) and A6 a) that there is a 'strong' positive correlation between the temperature at the inner surface of the fuel pellet and the outer diameter of the fuel rods.

The maximum cladding temperature has a 'strong' positive correlation with the initial outer diameter of the cladding and a 'strong' negative one with the initial inner cladding diameter There is also a 'strong' positive correlation between the gap thermal diameter and the initial cladding inner diameter [Figs. A3 d) and A6 d)]. This result is consistent with the heat conduction equation.

The temperature of the coolant has a 'very strong' positive correlation with the initial outer cladding diameter. This resulted in a 'strong' positive correllation with the cladding thickness [Figs. A3 c) and A6 c)].

The variation of the outer cladding diameter in case of UO_2 fuel rod shows 'strong' negative correlation with the initial value of the inner cladding diameter [gap thickness, Fig. A3 e)]. It is compensated with 'strong' positive cladding thickness correlation. In the case of $UO_2 - Gd_2O_3$ fuel rod, the correlation of the initial diameter with the gas pressure is positive and 'very strong' [Fig. A6 e)]. The activated Gd_2O_3 model in our FEMAXI calculations is based on Fukushima et al, (1982);

The gas pressure in both fuel rods shows 'very strong' positive dependence on their initial values. The positive dependence of the gas pressure on the inner cladding diameter is 'average' for UO_2 and 'weak' for $UO_2 - Gd_2O_3$ fuel rod [Figs. A3 f) and A6 f)].

Based on the obtained results, one can observe that the nonparametric statistical analysis follows and reveals the same relations that we already know from thermal and mechanical physics. It demonstrates the applicability of the statistical analysis to the fuel rod behavior.

The minimal DNBR during the fuel cycle in the reactor core is observed at the upper half of the reactor core (Figs. 5&6). The most pessimistic DNBR for UO_2 fuel rod is1.9 at 300 day of the irradiation and for $UO_2 - Gd_2O_3$ fuel rod is 2.0 at 350 day of the irradiation.

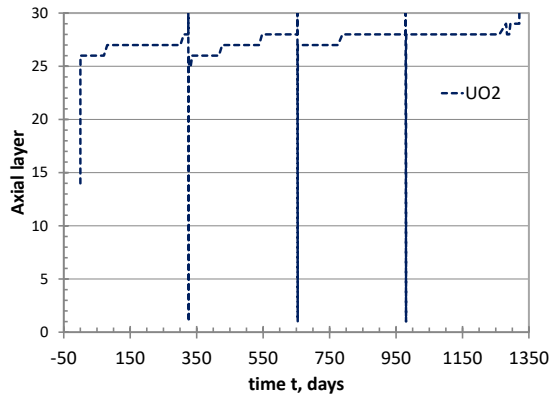

Fig. 5 Axial layer of UO_2 fuel rod with estimated CHFR.

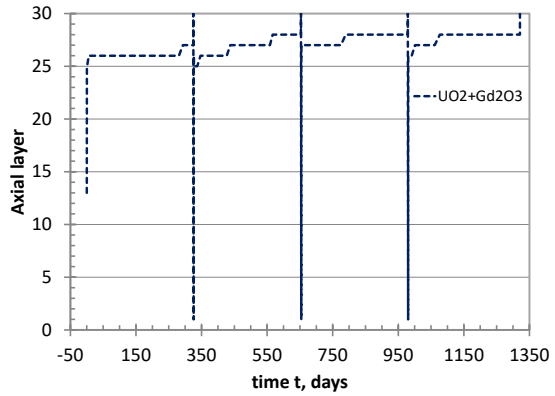

Fig. 6 Axial layer of $UO_2 - Gd_2O_3$ fuel rod with estimated CHFR.

The uncertainty analysis proves to be very promising in evaluation of the safety margins of nuclear fuel during normal plant operation.

Currently, in practical analyses, often an approach, called engineering sensitivity study (ESS) is applied, where the values of the input parameters are varied based on expert judgment in order to get a conservative estimation of the investigated parameters. We compared the SUSA bounding curves with the calculations of two sets of input data based on the engineering judgment. The temperature at the inner surface of the fuel pellet is the output parameter under concern (Figs B1&B2). The calculation with FEMAXI-6 for a vector with nominal values reveals this output parameter response (given in Figs B1&B2) to the input parameters.

We performed the ESS by selection of input values, suitable to obtain the bounding temperatures at the inner surface of the fuel pellets:

(1) For the highest values: the outer fuel diameter was selected to be at the lower limit of its uncertainty range $[d_{fuel}^{out}(UO_2)/d_{fuel}^{out}(UO_2 - Gd_2O_3)]$. We selected the remaining input parameters at their upper limit of uncertainty ranges, Table 1.

(2) For the lowest values: we did the opposite to (1).

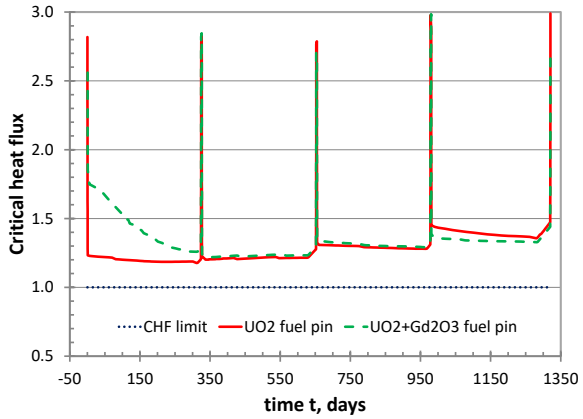

Fig. 7 CHFR for two cases: solid red line shows UO_2 fuel rod; green dashed line represents $UO_2 - Gd_2O_3$ fuel rod; blue dotted line shows the limit.

In Figs. B1 and B2 the results for the temperature in the inner surface of the cladding obtained from the ESS are shown together with the nominal parameters curve and with the SUSA uncertainty results. The

ESS bounding range is significantly narrower than the SUSA limiting curves. For the period from 0 to 500 day both ESS curves are higher than the nominal curve. This result demonstrates that it is difficult to choose the initial values of the input parameters from their uncertainty range in such a way that they definitely lead to a conservative estimation. Figures B1 & B2 demonstrate the advantage of uncertainty methods over ESS.

4 COMMENTS AND CONCLUSIONS

The presented in the paper approach, for uncertainty and sensitivity analysis, is used in the evaluation of nuclear installation safety at abnormal events (see for example Strydom, 2010). The current study demonstrates its successful application for the analysis of the influence of the fuel initial uncertainties on its condition during normal operation.

The FEMAXI-6 computer code was developed for the analysis of PWR fuel but our current verification showed that it can be applied also for evaluation of VVER-1000 fuel rods after preparation of a suitable input data set.

The geometrical and material uncertainties influence the mechanical parameters, such as thickness of the gap between the cladding and the fuel pellet, cladding outer diameter etc. Their influence on the heat transferring process is insignificant. The large thermal capacity of the fuel suppresses the significant temperature variation at the outer side of the fuel pellets. The heat transferred to the coolant is weakly affected.

The estimation of the fuel safety margins to the CHF shows that in the most unfavorable case, CHF is not achieved. Therefore, we draw the conclusion that the entire reactor core in these conditions does not exceed the limits for normal operation.

REFERENCES

Conover, W. J., 1999. *Practical Nonparametric Statistics*, 3rd edition, John Willey and Sons Inc., 584 pp.

Esser, E., Koc, H., Gokbult, M. and Gursoy G., 2014. Estimations of Heat Capacities for Actinide Dioxide: UO_2, NpO_2, ThO_2, and PuO_2, *Nuclear Engr. And Tech.*, 46 (6), 863–868

Fukushima, S., Ohmichi, T., Maeda, A. & Watanabe, H., 1982. The Effect of Gadolinium Content on the Thermal Conductivity of Near-Stoichiometric $(U,Gd)O_2$ Solid Solutions, *J. Nucl. Mater.* 105, 201–210.

Glaeser, H., 2008. GRS Method for Uncertainty and Sensitivity Evaluation of Code Results and Applications, *Sci. and Technol of Nucl. Inst.*, 2008, 1–7.

IAEA, 2013. *Improvement of Computer Codes Used for Fuel Behaviour Simulation-FUMEXIII*, IAEA-TECDOC-1967, IAEA, 142 pp.

Kamenov, K., 2017. *Computed Neutron-Physical Characteristics of Stationary Fuel Loadings with 42/48 fresh Fuel Assemblies TVSA for VVER-1000 of Units 5 and 6 of Kozloduy NPP*, 11.35.ОБ.УС.НФХ.18-25/0, 126 pp.

Kloos, M., 2015. *Mean features of the tool SUSA 4.0 for uncertainty and sensitivity analyses*, Safety and Reliability of Complex Engineered Systems: ESREL 2015, ISBN-978-1-138-02879-1, 2533-2560, Taylor & Francis Group, London, Luca Podofillini, Bruno Sudret,Bozidar Stojadinovic, Enrico Zio, Wolfgang Kröge.

Kovbacenko, Y., 2016. Comparative Analysis of VVER-1000 Westinghouse and TVEL Spent Fuel Capability, *Univ. J. of Phys. and Appl.* 10(4), 105–109.

Molchanov, V., 2009. Nuclear Fuel for VVER reactors. Actual State and Trends, in *Proceedings 8-th Intl. Conf. on VVER Fuel Performance, Modeling and Experimental Support, 27.09–02.10.*, Helena Resort, Bulgaria.

Odeychuk, N.P., Sidorenko, S.A., Bolshak, A.I.,Slabospitskaya, E.A., & Roenko, N.M., 2008. Some Characteristics of Experimental Bilayer Urane-Gadolimium Pellets, *Voprosy Atomnoy Nauki I Tehniki*, 1, 133–135.

OECD, *Nuclear Energy Agency*," OECD, 2017. Available: http://www.oecd-nea.org/tools/abstract/detail/nea-1080/.

Onufriev, E., 2005. Design and Fabrication of Nuclear Fuel for WWER And RBMK Reactors, in *Workshop on "Modelling and Quality Control for Advanced and Innovative Fuel Technologies, 14-25 November 2005*, The Abdu Salam International Centre for Theoretical Physics, Trieste, Italy.

Passage, G., Stefanova, S., Scheglov, A., Proselkov, V., 19–23 September 2005. *Comparative calculations and operation-to-PIE data juxtaposion of the ZapNPP, WWER-1000 FA-E0325 fuel rods after 4 years of operation up to ≈49 MWd/kgU burnup*, Proceedings of the 6th International Conference on WWER Fuel Performance, Modelling and Experimental Support, Albena, Bulgaria.

Passage, G., Mandev, I. & Stefanova, S., 27 September – 03 October, 2009. *Extension of the* FEMAXI-6 Code to Analyse WWER Fuel Rods Using the IFPE Data Base, *Proceedings of the 8-th International Conference WWER Fuel Performance, Modelling and Experimental Support*, Helena Resort, Bulgaria.

Pernica, R.& Cizek, J. 1994. *PG general correlation of CHFR and statistical evaluation results*, Ustav Jaderneho Vyzkumu a.s., Rez (Czech Republic), 45pp.

Schrire, D., Kindlund, A. & Ekberg, P., 1998. *Solid Swelling of LWR UO_2 Fuel*, HPR-349/22, Lillehammer, Norvay.

Stefanova, S., Pasage, G., Mandev, I. & Stefanova, M., 2012. Calculation of Thermomechanical Behavior of Nuclear Fuel with TRANSURANUS Computer Code with Usage of Boundary Conditions Obtained with Calculation of Reactor Core Loads, *Report*, INRNE, BAS, Sofia.

Strydom, G., 2010. *Use of SUSA in Uncertainty and Sensitivity Analysis for INL VHTR Coupled Codes*, *INL/EXT-10-19023*, Idaho National Laboratory, Next Generation Nuclear Plant Project Idaho Falls, Idaho 83415, 29pp.

Suzuki, M., Saitou, H., 2006. *Light Water Reactor Fuel Analysis Code. FEMAXI-6 (Ver.1). Detailed structure and user's manual*, Japan Atomic Energy Agency, Tokyo, JAEA-DATA/CODE–2005–003, 425 pp.

Tong, L., 1997. *Boiling Heat Transfer and Two-Phase Flow*, 2nd edition, ISBN 1-56032-485-6, John Wiley and Sons Inc., New York, Lynne Lackenbach & Holy Seltzer.

Udagawa Y, Suzuki M., Fuketa T., 2007. Analysis of MOX fuel behavior in Halden reactor by FEMAXI-6 code, *J. Nucl. Sci. Technol.,* 44(8), 1070–1080.

USNRC, TREE NUREG-1005, MATPRO-09, 1976. *A Handbook of Materials Properties for Use in the Analysis of Light Water Reactor Fuel Rod Behavior*, USNRC TREE NUREG-1005.

Wiesenack, W. & Tverberg, T., 2000. Thermal Performance of High Burnup Fuel – In-pile Temperature Data and Analysis, in *Proceedings 2000 Int. Topical Meeting on LWR Fuel Performance*, Park City, USA.

Wilks, S., 1941. Determination of sample sizes for setting tolerance limits, *Annals of Math. Statistics*, 1(1), 91–96.

Wilks, S., 1942. *Statistical prediction with special reference to the problem of tolerance limits, Annals of Math. Stats.*, 13(4), 400–409.

Wolfram Research, Inc., 2016. *Mathematica, Version 11.0*, Wolfram Research, Inc, Champaign, Illinois, Software.

Yamji, A., Suzuki, M., & Okubo, T., 2009. FEMAXI-6 Code Verification with MOX Fuels Irradiated in Halden Reactor, *J. Nucl. Sci. and Technol*, 46(12), 1152-1161.

.

APPENDIX

A.1. EVALUATED OUTPUT UNCERTAINTIES

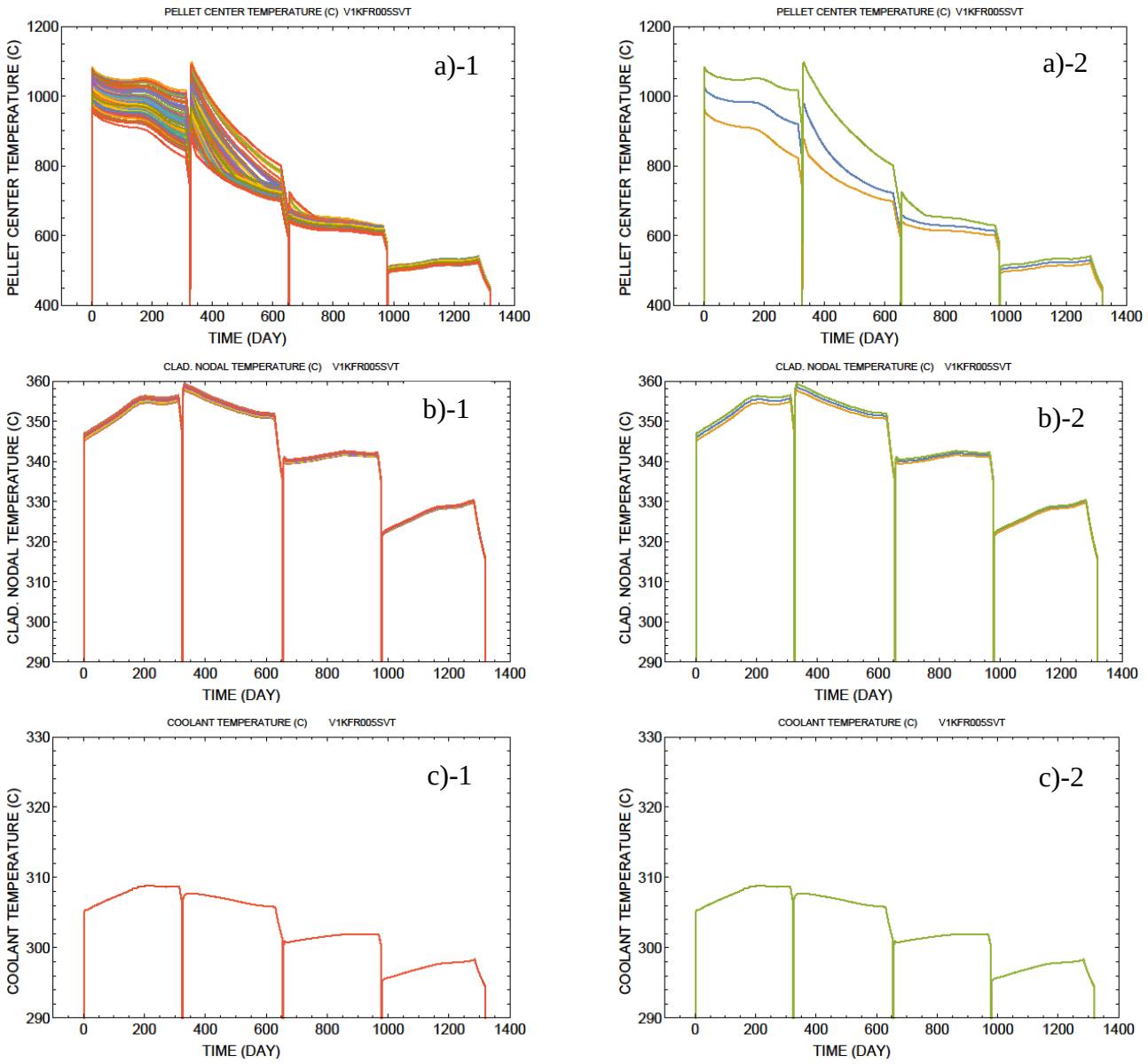

Fig. A1 Output parameters from calculations of UO_2 fuel rod (the axial layer No.14), after variation of the initial geometrical and material parameters, in ranges defined in Table 1: a)-1 temperature at the inner surface of the fuel pellet; a)-2 maximal, average and minimal temperature at the inner surface of the fuel pellet; b)-1 temperature in the cladding; b)-2 maximal, average and minimal temperatures in the cladding; c)-1 coolant temperature; c)-2 maximal, average and minimal coolant temperature.

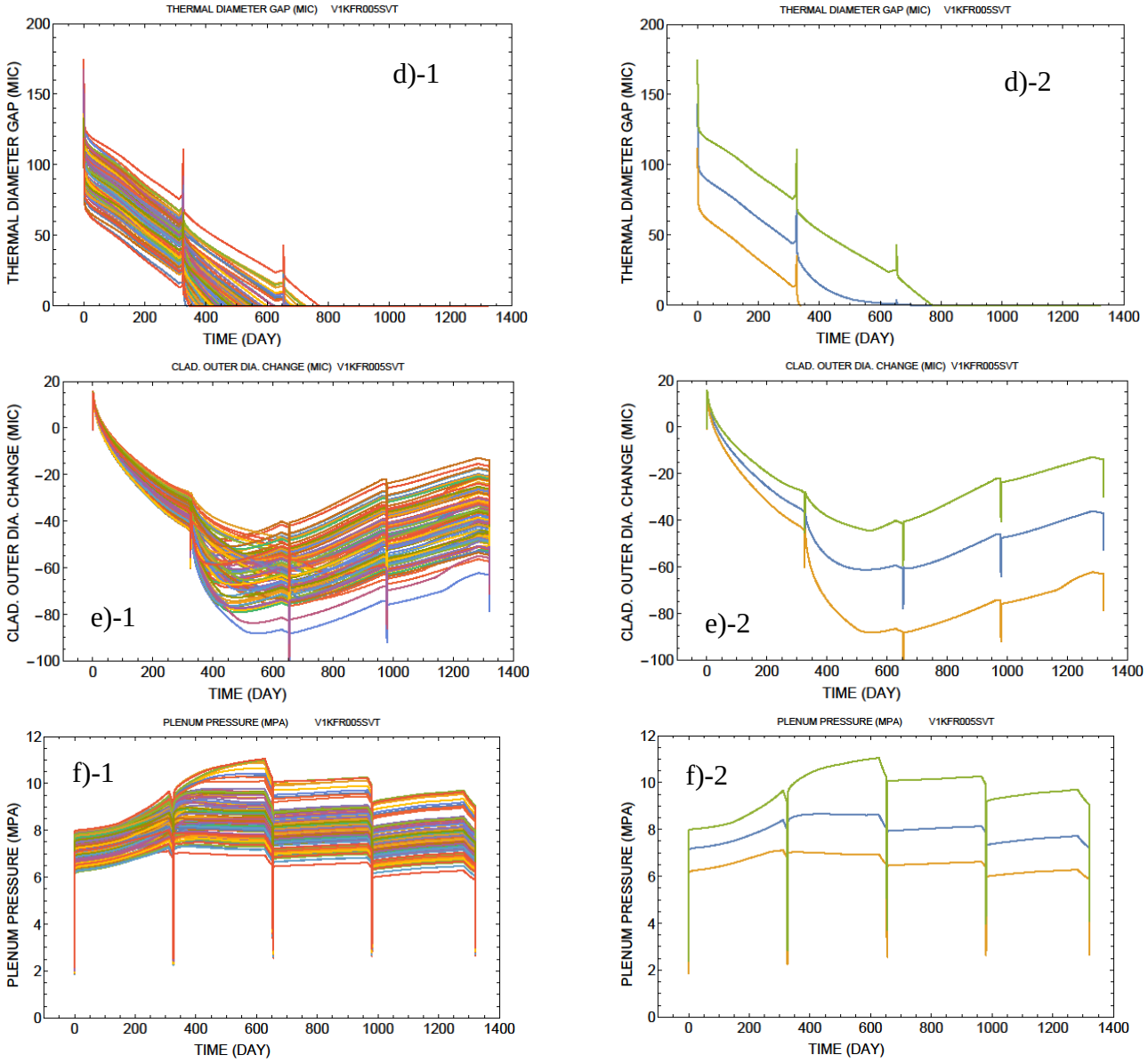

Fig. A2 Output parameters from calculations of UO_2 fuel rod (the axial layer No.14), after variation of the initial geometrical and material parameters, in ranges defined in Table 1: d)-1 thickness of gap between cladding and fuel pellet; d-2) maximal, average and minimal gap between cladding and fuel pellet; e)-1 cladding outer diameter; e)-2 maximal, average and minimal values of cladding outer diameter; f)-1 gas pressure in fuel element; f)-2 maximal, average and minimal values of pressure in the fuel element.

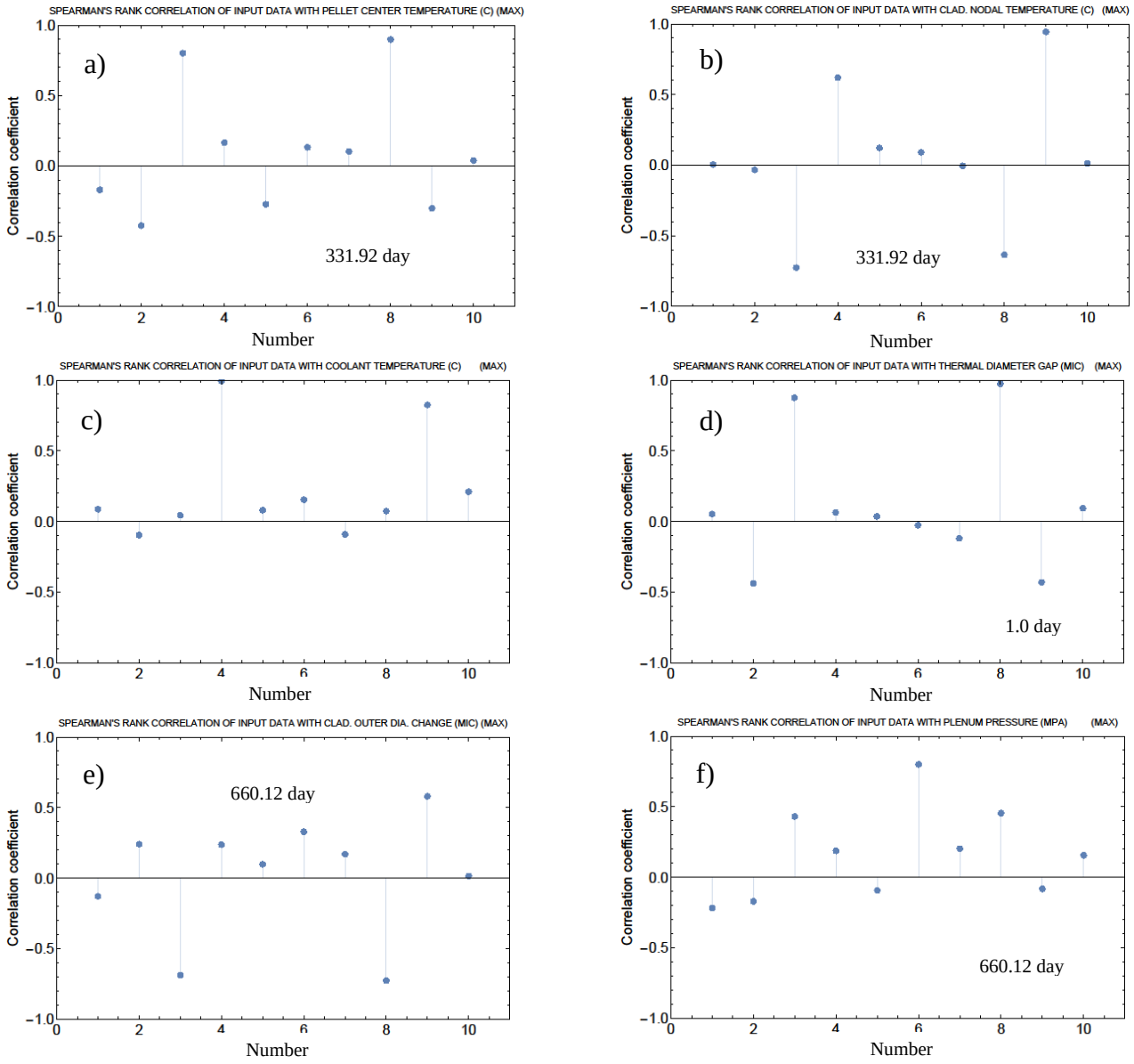

Fig. A3 Estimation by Spearman's correlation coefficient the statistical relationships between the initial values of geometrical and material parameters of UO_2 fuel rod and calculated (output) values of selected parameters for axial layer No. 14: a) temperature at the inner surface of the fuel pellet; b) temperature in the cladding; c) coolant temperature; d) thickness of the gap between the cladding and the fuel pellet; e) outer diameter of the cladding; f) gas pressure in the fuel rod. The horizontal axes of all graphs contain the following input parameters: 1- initial fuel pellet gap diameter; 2- initial fuel pellet outer diameter; 3- initial cladding inner diameter; 4- initial cladding outer diameter; 5- initial fuel pellets material density; 6- initial gas pressure in fuel rod; 7-initial thickness of fuel pellets; 8- initial thickness of gap between the cladding and the fuel; 9- initial thickness of the cladding wall; 10- averaged Spearman's correlation coefficient.

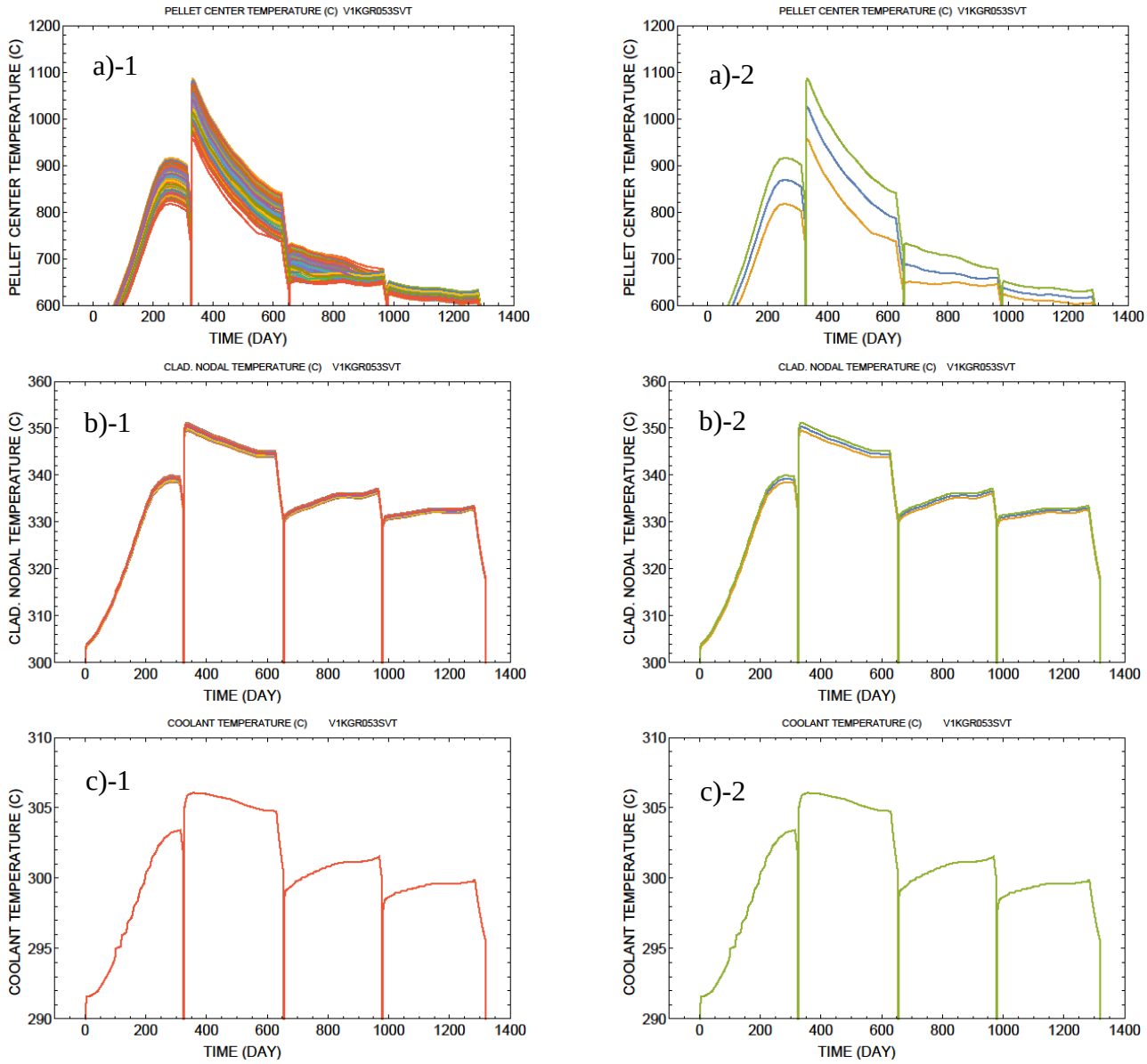

Fig. A4 Output parameters from calculations of $UO_2 - Gd_2O_3$ fuel rod (the axial layer No.14), of the initial geometrical and material parameters, in ranges defined in Table 1: a)-1 temperature at the inner surface of the fuel pellet; a)-2 maximal, average and minimal at the inner surface of the fuel pellet; b)-1 temperature in the cladding; b)-2 maximal, average and minimal temperatures in the cladding; c)-1 coolant temperature; c)-2 maximal, average and minimal coolant temperature.

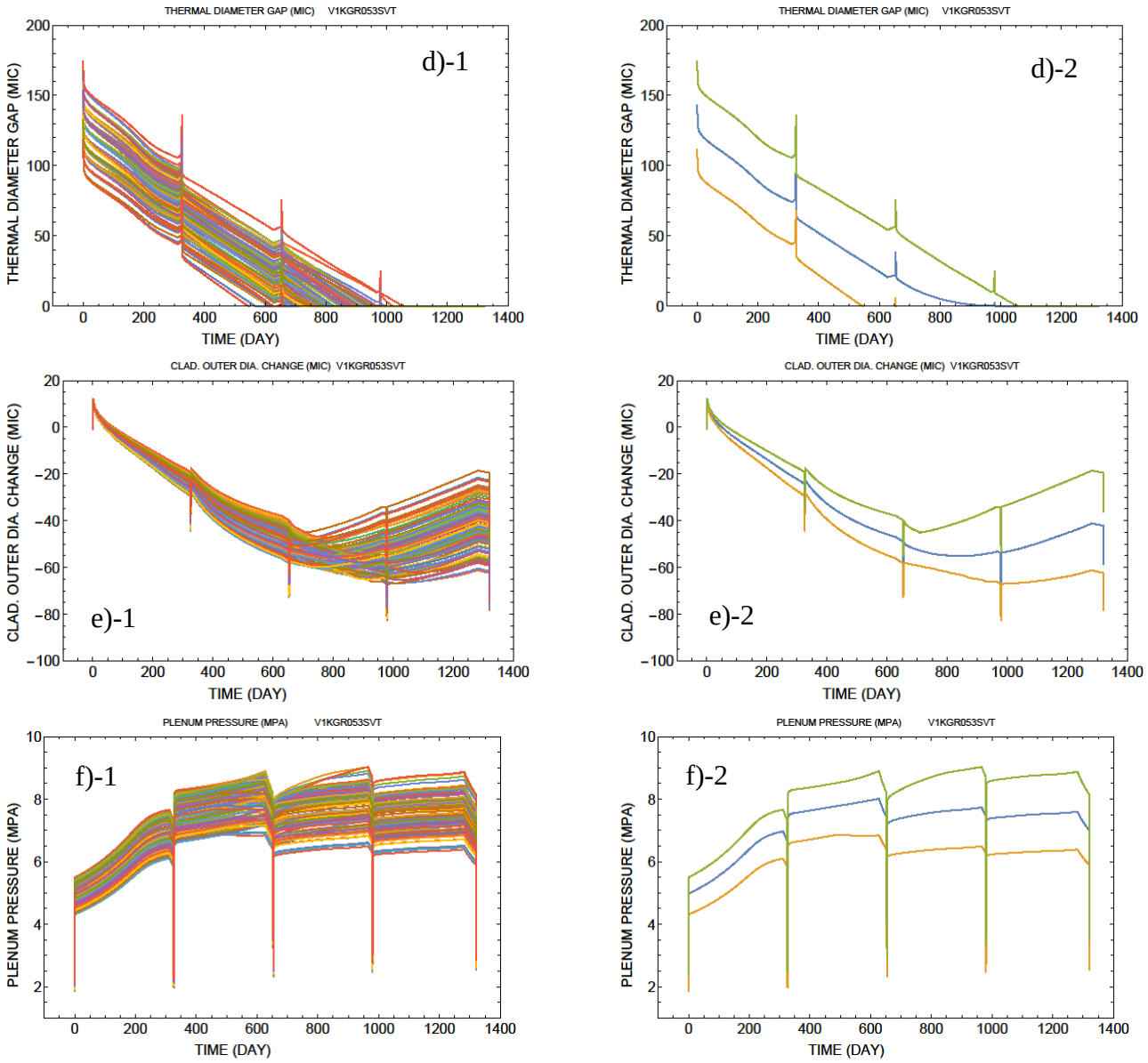

Fig. A5 Output parameters from calculations of $UO_2 - Gd_2O_3$ fuel rod (the axial layer No.14), of the initial geometrical and material parameters, in ranges defined in Table 1: d)-1 thickness of the gap between the cladding and the fuel pellet; d)-2 maximal, average and minimal gap between the cladding and the fuel pellet; e)-1 cladding outer diameter; e)-2 maximal, average and minimal values of cladding outer diameter; f)-1 gas pressure in the fuel element; f)-2 maximal, average and minimal values of pressure in the fuel element.

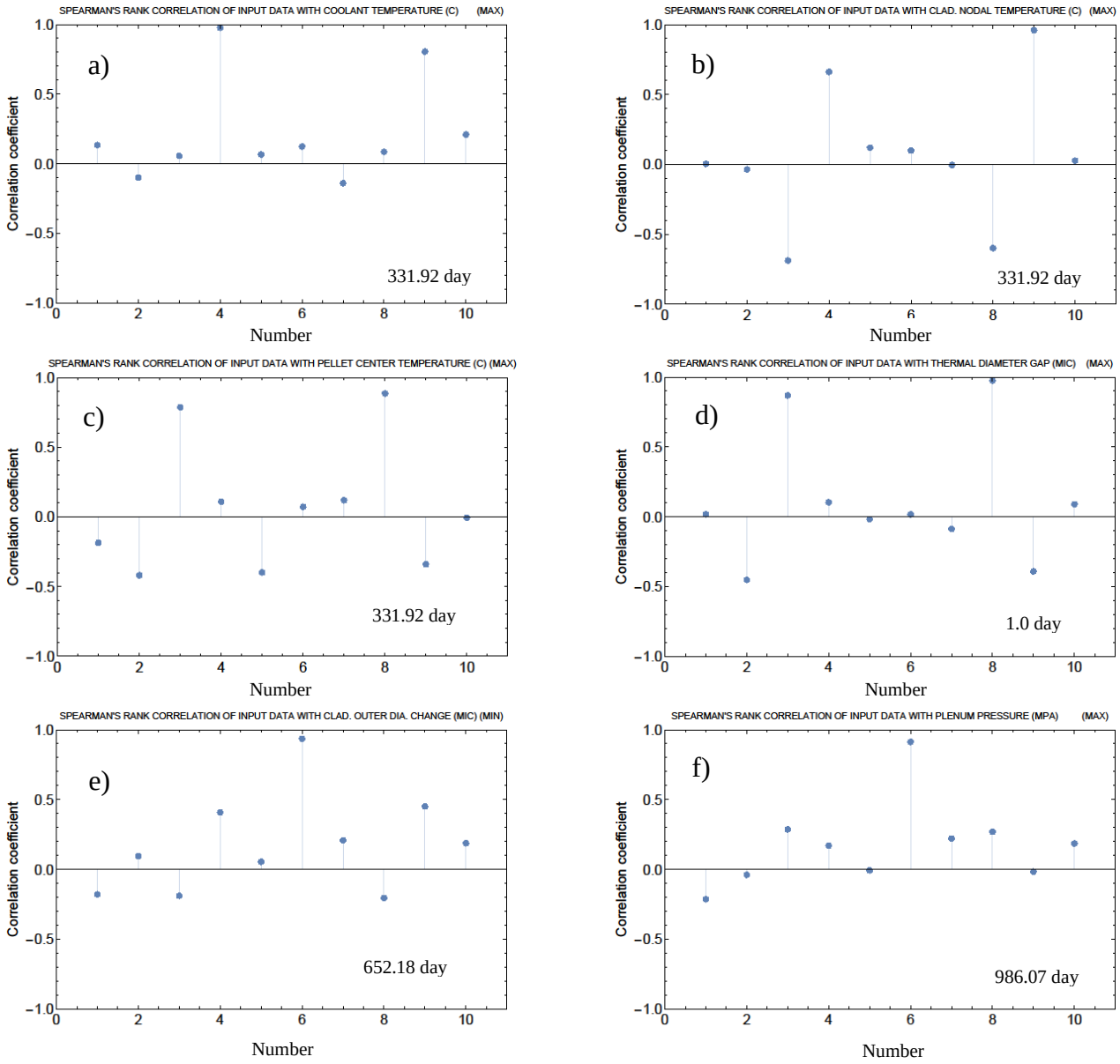

Fig. A6 Estimation by Spearman's correlation coefficient the statistical relationships between the initial values of geometrical and material parameters of $UO_2 - Gd_2O_3$ fuel rod and calculated (output) values of selected parameters for axial layer No. 14: a) temperature at the inner surface of the fuel pellet; b) temperature in the cladding; c) coolant temperature; d) thickness of the gap between the cladding and the fuel pellet; e) outer diameter of the cladding; f) gas pressure in the fuel rod. The horizontal axes of all graphs contain the following input parameters: 1- initial fuel pellet gap diameter; 2- initial fuel pellet outer diameter; 3- initial cladding inner diameter; 4- initial cladding outer diameter; 5- initial fuel pellets material density; 6- initial gas pressure in fuel rod; 7-initial thickness of fuel pellets; 8- initial thickness of gap between the cladding and the fuel; 9- initial thickness of the cladding wall; 10- averaged Spearman's correlation coefficient.

B. SENSITIVITY AND UNCERTAINTY ANALYSIS

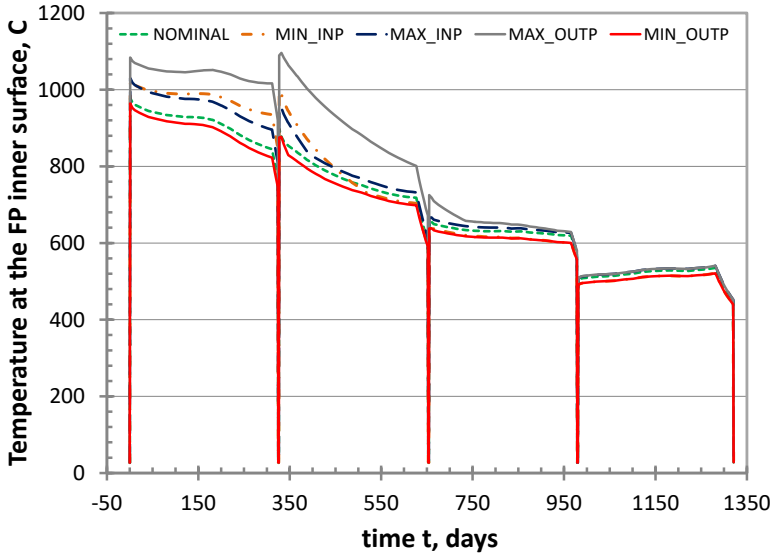

Fig. B1 Temperature at the inner surface of the UO_2 fuel pellet (FP): min_INP- all input parameters are selected to be at the lower edge of their uncertainty range beside the fuel pellet outer diameter which is selected to be at the maximum; max_INP- all input parameters are selected to be upper edge of the range beside the fuel pellet outer diameter, selected to be at the minimum; NOMINAL- nominal values of input parameters; MIN_OUTP and MAX_OUTP bounding curves obtained by SUSA.

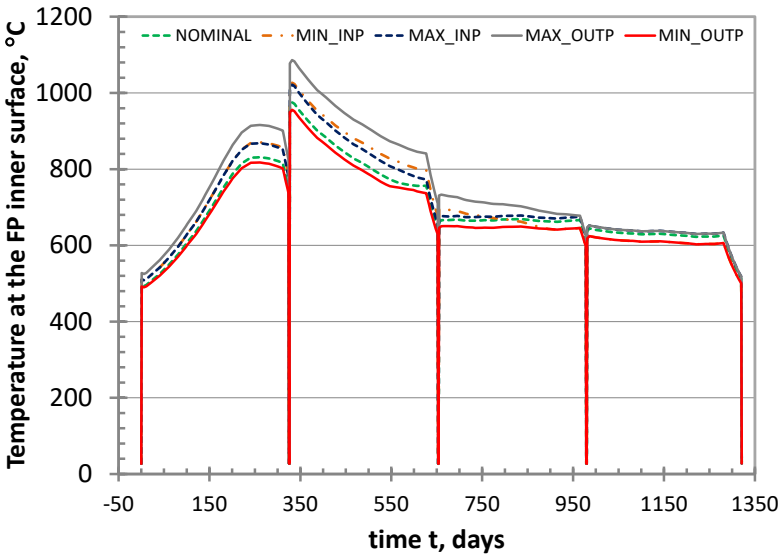

Fig. B2 Temperature at the inner surface of the $UO_2 - Gd_2O_3$ fuel pellet (FP): min_INP- all input parameters are selected to be at the lower edge of their uncertainty range beside the fuel pellet outer diameter which is selected to be at the maximum; max_INP- all input parameters are selected to be upper edge of the range beside the fuel pellet outer diameter, selected to be at the minimum; NOMINAL- nominal values of input parameters; MIN_OUTP and MAX_OUTP bounding curves obtained by SUSA.